HHS Public Access

Author manuscript

J Invest Dermatol. Author manuscript; available in PMC 2022 December 09.

Published in final edited form as:

J Invest Dermatol. 2018 December ; 138(12): 2531–2539. doi:10.1016/j.jid.2018.06.186.

HSP70i$_{Q435A}$-Encoding DNA Repigments Vitiligo Lesions in Sinclair Swine

Steven W. Henning[1,2], **Manuel F. Fernandez**[1], **James P. Mahon**[1], **Richard Duff**[3], **Farshid Azarafrooz**[3], **José A. Guevara-Patiño**[1,4], **Alfred W. Rademaker**[5], **Andrew L. Salzman**[6], **I. Caroline Le Poole**[1,2,7]

[1]Oncology Research Institute, Loyola University, Chicago, Illinois, USA

[2]Department of Dermatology, Northwestern University, Chicago, Illinois, USA

[3]Comparative Medicine Facility, Loyola University, Chicago, Illinois, USA

[4]Department of Surgery, Loyola University, Chicago, Illinois, USA

[5]Department of Preventive Medicine, Northwestern University, Chicago, Illinois, USA

[6]Salzman Group, Beverly, Massachusetts, USA

[7]Departments of Pathology, Microbiology and Immunology, Loyola University, Chicago, Illinois, USA

Abstract

Human HSP70i$_{Q435A}$ carries a single amino-acid modification within the dendritic cell activating region and tolerizes dendritic cells in vitro. The underlying DNA was used to prevent and treat disease in vitiligo mouse models through reduced dendritic cell activation and diminished skin T-cell infiltration, suggesting the same may be useful for patients. Physiologic differences between mouse and human skin then called for studies in large animals with human-like skin. We established the efficiency of DNA jet injection into swine skin before subcloning *HSP70i$_{Q435A}$* into clinically suitable vector pUMVC3. Vitiligo lesions in Sinclair swine were treated with plasmid DNA to measure changes in depigmentation, T-cell infiltration, expression of HSP70i in skin, serum HSP70i, and anti-HSP70i serum titers. Remarkable repigmentation following HSP70i$_{Q435A}$-encoding DNA treatment persisted throughout the 6-month follow-up period. Repigmentation was accompanied by an initial influx of T cells accompanied by increased CD4/CD8 ratios, waning by week 15. Melanocytes spanned the border of repigmenting skin, suggesting that melanocyte repopulation precedes skin melanization. Serum titer fluctuations were not treatment-associated. Importantly, treatment did not interfere with melanoma immunosurveillance. These data encourage clinical testing of *HSP70i$_{Q435A}$*.

Correspondence: I. Caroline Le Poole, Lurie Comprehensive Cancer Center, Room 3-121, Northwestern University, 303 East Superior Street, Chicago, Illinois 60611, USA. caroline.lepoole@northwestern.edu.

SUPPLEMENTARY MATERIAL

Supplementary material is linked to the online version of the paper at www.jidonline.org, and at https://doi.org/10.1016/j.jid.2018.06.186.

INTRODUCTION

In vitiligo, depigmentation is associated with perilesional T-cell infiltration. Cytotoxic T cells reactive with melanosomal antigens are primarily responsible for progressive melanocyte loss (Strassner and Harris, 2016). The disease can be triggered by different forms of stress, and skin Koebnerization is common, particularly in confetti-like depigmentation (Kundu et al., 2018;Sosa et al., 2015). Thus, stress proteins might mediate cutaneous depigmentation. Indeed, inducible HSP70 (HSP70i) is a central player in vitiligo (Mosenson et al., 2013a). HSP70i was upregulated in vitiligo skin, preferentially localizing to nuclei (Abdou et al., 2013). HSP70i-encoding DNA markedly enhanced vitiligo development in mice, whereas vitiligo does not occur in HSP70i knockout animals (Mosenson et al., 2012). Moreover, melanocytes from pigmented patient skin displayed increased secretion of HSP70i after stress compared to control melanocytes (Mosenson et al., 2014). In turn, HSP70i can activate dendritic cell (DC) subsets including plasmacytoid DCs (Jacquemin et al., 2017). These events help explain the enhanced recruitment of CXCR3-expressing T cells to the skin (Boniface et al., 2018). Antibodies to CXCR3 can interfere with vitiligo development in mice (Richmond et al., 2017). Treatment of vitiligo has proven particularly challenging, given the two-step requirement for halting ongoing autoimmune responses, as well as driving melanocyte repopulation of depigmented skin. Despite these challenges, new treatment strategies are on the horizon (Frisoli and Harris, 2017).

Blocking HSP70i activity might offer an effective means to interfere with vitiligo development. To develop this intervention, a site within the molecule critical to DC activation was identified by aligning HSP70i cDNA to its bacterial homologue DnaK, leading to the identification of a sequence encoding an 11 amino-acid stretch responsible for human DC activation by site-directed mutagenesis (Mosenson et al., 2013b). A version with a strategically placed, single amino-acid change was selected for further investigation, and plasmid DNA encoding $HSP70i_{Q435A}$ proved capable of preventing and treating vitiligo in mouse models of vitiligo (Mosenson et al., 2013b). Central to this finding was the immune tolerizing activity of $HSP70i_{Q435A}$. The modified HSP tolerized DCs of mouse and human origin in vitro. Upon introduction into the skin of vitiligo-prone mice, the DNA construct interfered with infiltration of melanocyte-reactive T cells and enhanced the Eomes to T-bet ratio among T cells, an observation likewise made when comparing T cells′ control to vitiligo patient blood (Mosenson et al., 2013b).

These findings warranted further investigation of the $HSP70i_{Q435A}$-encoding construct applied to human-like skin because mouse and human skin differ (Jung and Maibach, 2015). In particular, multilayered human epidermis calls for a different means to introduce DNA. Swine commonly serve to measure the efficacy of topical drug applications, and Sinclair swine were used to measure treatment efficacy here (Okomo-Adhiambo et al., 2012). These swine develop melanomas that regress by immune surveillance, accompanied by an influx of T cells (Morgan et al., 1996). Such animals will ultimately develop progressive depigmentation, and resulting lesions were included in the current studies to test $HSP70i_{Q435A}$ and its ability to treat vitiligo.

Introducing DNA to the skin can be approached by several techniques. The gene gun can effectively introduce DNA to the skin, but this method is not readily translatable to human applications. Alternatively, tattooing, electroporation, dermarolling, and jet injection can be used (Kim et al., 2012). The two most feasible methods were compared to select one for application to Sinclair swine with vitiligo and melanoma.

Animals were subjected to perilesional jet injection with DNA encoding HSP70i$_{Q435A}$ or diluent. Changes in treated and distant lesional sizes were measured by image analysis, and perilesional biopsies and serum samples were taken frequently to track melanocytes or CD4 and CD8 T cells in skin and measure HSP70 and anti-HSP70i antibody titers. Changes in cutaneous melanoma lesions were identified. Experiments provide insight into the treatment potential of jet-injected HSP70i$_{Q435A}$-encoding DNA applied to human-like vitiligo skin.

RESULTS

Sinclair swine are suited to model vitiligo development

Vitiligo lesions in Sinclair swine exhibit striking similarity to human lesions as shown in Supplementary Figure S1a (online) compared to Supplementary Figure S1b. As depigmentation and repigmentation are defined by melanocyte abundance, it is significant that the distribution of basal melanocytes is similar to that observed in human skin, as shown in Supplementary Figure S1c compared to Supplementary Figure S1d. This also demonstrates that swine melanocytes (arrows) are detectable using antibody Ta99 to TRP-1 (Thomson et al., 1985). Koebnerization is exemplified in swine with skin trauma after earmarking (Supplementary Figure S1e) and after an altercation with another animal (Supplementary Figure S1f). This disease feature is also reported by patients. Note vitiligo surrounding the skin incisions in Supplementary Figure S1e. This justifies the use of Sinclair swine to test HSP70i$_{Q435A}$ as a vitiligo treatment.

Jet injection of plasmid DNA can drive expression of the encoded protein in skin

A plasmid encoding the ZsGreen marker was used to compare the efficacy of skin introduction methods. DNA was applied by jet injection or by microneedles using a titanium dermaroller. A punch biopsy was taken and homogenized. Among live cells, the percentage of ZsGreen^{+} cells was measured after 96 hours (Figure 1a–1c). No significant expression was observed after dermarolling, but 26.5% of cells expressed ZsGreen following jet injection. This experiment was repeated twice, and jet injection was superior both times. This supported jet injection to introduce HSP70i$_{Q435A}$-encoding DNA into human-like skin to evaluate therapeutic effects. The staining score representing HSP70i nuclear staining in vitiligo perilesional skin is downregulated by the end of DNA treatment at t = 3 weeks, but not by vehicle treatment, measured in one-tailed *t* test with Welch′s correction ($P < 0.05$) (Figure 1d). A typical change in staining score is exemplified in Figure 1e.

HSP70i$_{Q435A}$ treatment repigments vitiligo skin in Sinclair swine

Treated vitiligo lesions received four doses of *HSP70i$_{Q435A}$* weekly for 4 weeks, and changes in lesional size were quantified for another 6 months. Image analysis was used to measure the surface area of treated lesions (n = 7), not including melanoma area.

Changes were likewise measured for distant, non-biopsied lesions on treated swine when available (n = 7). The mode of measurement is shown in Figure 2a. Individual changes in lesional size are shown in Supplementary Figure S2 (online). Changes were compared to vehicle-treated lesions from separate swine (n = 5). In Figure 2b, the difference in slope between DNA-treated (−12.5), distant (−14.2), and control lesions (31.9) was highly significant ($P < 0.0001$). This treatment effect is further supported by a significant reduction in size of both DNA-treated and distant lesions over time ($P < 0.0001$ for both). By contrast, repigmentation was not observed in distant lesions that were biopsied, as shown in Supplementary Figure S3 (online). In Figure 2c, repigmentation is displayed proportionate to the pretreatment lesional size in pie charts differentiating depigmentation from partial and near-complete repigmentation. The majority of lesions followed in treated swine responded by moderate to complete repigmentation, whereas vehicle-treated lesions mostly depigmented over time. This important observation prompted studies to verify melanocyte repopulation of repigmenting skin.

Melanocyte repopulation precedes skin repigmentation in *HSP70i*$_{Q435A}$-treated skin

Sequential biopsies spanning the border of repigmenting skin were evaluated for the presence of melanocytes. In Figure 3a, swine perilesional skin is shown 6 months after the last DNA jet injection. In the Figure 3b, melanocytes are detectable beyond the pigmented borders. As this lesion repigmented over time, the presence of lesional melanocytes suggests that pigment cell repopulation precedes repigmentation. In Figure 3c, melanocyte densities in the depigmented epidermis are compared to those observed in the pigmented epidermis from the same perilesional biopsies. In Figure 3d, biopsies from phosphate buffered saline (PBS)–treated lesions also exhibit some remaining melanocytes. Overall melanocyte density is approximately 64% reduced in perilesional depigmented skin. These data further support the presence of some melanocytes in depigmented perilesional skin independent of disease status. Additionally, the results reinforce the similarity between swine and human skin, as melanocytes are readily detectable as basal TRP-1^{+} cells. The results prompted us to study whether repigmentation correlates with resolution of T-cell infiltrates.

T-cell infiltration is reduced during the repigmentation process

Biopsies from DNA-treated lesions were analyzed for T-cell infiltration before and after treatment. It is expected that T-cell numbers will vary, as lesions may experience different stages of progression at treatment onset. In Figure 4a, example stainings at three time points are shown for CD3 detection above, and for CD3(red)/CD8(green) double staining to discern the cytotoxic (double stained) and helper/suppressor (single stained) subsets below. Fluctuations in T-cell infiltrates and in the CD4/CD8 ratio are shown in Figure 4b. A significant decrease in T cells is shown 3 months after DNA treatment in Figure 4c. A marked trend toward increased T-cell infiltration was apparent during and immediately after DNA treatment, suggesting that immunosuppressive T cells may outnumber CD8^{+} cytotoxic effectors. CD3/CD8 double stainings served to quantify CD4/CD8 ratios (Figure 4c). The CD4/CD8 ratios followed the same pattern as overall T-cell infiltration, revealing an initial increase at week 7, followed by leveling of the ratio. Limited FoxP3 staining was observed (Supplementary Figure S4 online), thus initially infiltrating CD4 T cells may in part be

Th2 cells supporting a drive toward humoral responses, and we reasoned that an antibody response to HSP70i$_{Q435A}$ may arise.

DNA treatment does not elicit humoral responses to HSP70

We expected that an increase in HSP70 expression may elicit humoral responses, as reported previously for mice (Mosenson et al., 2013b). Anti-HSP70i antibodies could deplete soluble HSP70i and thereby prevent DC activation, possibly contributing to a therapeutic effect. We observed no increases in HSP70i titers in serum over time in response to treatment in a comparison to vehicle-treated swine in Figure 5a, which is not unexpected, given localized application of the *HSP70i$_{Q435A}$* construct. Similarly, there was no significant fluctuation in anti-HSP70i titers (Figure 5b). Thus, anti-HSP70i titers observed in gene gun–treated mice are unlikely to mediate reduced immune activation by depleting HSP70, supporting subsequent repigmentation. This is further corroborated by equal titers previously observed in response to wild-type or modified HSP70i in mice.

DNA treatment can support anti-tumor responses in treated swine

The surface area of melanoma tumors inside vitiligo lesions treated with DNA or PBS was quantified over time in Figure 6a. Remarkably, melanoma lesions treated with HSP70i$_{Q435A}$-encoding DNA significantly decreased in size when compared to PBS treated skin overall, though observed effects are due primarily to the presence of vitiligo. HSP70i found in the membrane of melanoma cells appears to lend itself to antibody-mediated cellular cytotoxicity (Shevtsov et al., 2018), while HSP70i generated by tumor cells may also incite continued recruitment of tumor reactive T cells. Such T cells were observed in both vehicle-treated and DNA-treated lesions (Figure 6b) at similar densities (Figure 6c). S100^{+} melanoma cells were propagated from tumor tissue at the end of the observation period from a DNA-treated lesion, indicating viable tumor tissue. Thus, a reduction in size represents true tumor shrinkage.

DISCUSSION

Vitiligo affects a large population of patients in need of treatment options (Frisoli and Harris, 2017). The DNA sequence encoding HSP70i$_{Q435A}$ has been developed to deactivate locally infiltrating DCs responding to cells under stress (Mosenson et al., 2013b). In stark contrast to unmodified HSP70i, which accelerates depigmentation, or to vector DNA, which does not affect disease progression, the HSP70i$_{Q435A}$–encoding DNA contained and reversed vitiligo in mouse models. For a future clinical application, it became important to select a skin introductory method applicable in patient settings (Apostolopoulos, 2016), and suited for human-like skin (Kim et al., 2012). What is indeed remarkable is the therapeutic success of naked DNA when administered by jet injection, as tested here. Such success will depend in part on properties of the plasmid backbone, confined by safety regulations. Approved use of the pUMVC3 plasmid is reported for clinical trials testing a treatment of ovarian, fallopian tube, and peritoneal cancers (ClinicalTrials.gov ID NCT03029611) and a trial for the treatment of breast cancer under NCT02780401. The plasmid dictates expression of the inserted gene under a CMV promoter, which might be silenced over time (Duan et al., 2012). The same promoter was involved in prior mouse studies, which likewise displayed

responses 6 months after plasmid application. Nevertheless, new depigmentation may be expected if a patient endures new episodes of stress (Harris, 2016). There is no reason for concern about limited efficacy of *HSP70i*$_{Q435A}$ upon retreatment, as some swine have likewise undergone sequential successful treatments.

Sinclair swine proved uniquely suited for vitiligo studies as developing lesions exhibit progressive loss of melanocytes as shown in patients (Le Poole et al., 1993). Though the kinetics of vitiligo development were not previously known, depigmentation will progress to varying extent and spontaneous repigmentation has not been reported (Misfeldt and Grimm, 1994). Interestingly, we observed some melanocytes in repigmenting perilesional skin. Such perilesional TRP1^{+} melanocytes may be indicative of ongoing repigmentation.

The combination of melanoma and vitiligo observed in Sinclair swine (Misfeldt and Grimm, 1994) is major histocompatibility complex (MHC)–associated (Blangero et al., 1996) and suggests T-cell–mediated immunity to antigen(s) shared by melanocytes and melanoma cells, also demonstrated in human melanoma patients developing vitiligo (Becker et al., 1999). Autoimmune vitiligo is likewise accompanied by ongoing immunity to melanosomal antigens, shown by in vitro assays (Wankowicz-Kalinska et al., 2003), tetramer analysis (Ogg et al., 1998) and TCR cloning experiments (Mantovani et al., 2003). Therapeutics should thus interfere with cutaneous T-cell activity, and HSP70i$_{Q435A}$ induced a significant reduction in T cells after treatment. CD4 T cells predominate immediately after treatment, suggesting regulatory T-cell infiltration. Reduced DC activation may be at play, whereas increased DC activity is expected under stress. This aligns with increased depigmentation in stressed porcine skin, and further supports the use of spontaneously depigmenting swine for therapeutic assessments (Bourneuf, 2017). Emotional stress may likewise contribute to vitiligo in this model as an impact of stress on depigmentation was recently shown in mice (Liao et al., 2017).

Successful treatment of vitiligo might be accompanied by reduced anti-tumor activity and, once T-cell responses to shared antigens are diminished, a concern for melanoma development can arise (Naveh et al., 2013). Here, the shrinking melanoma surface area within DNA-treated vitiligo lesions implies otherwise. The presence of vitiligo alone is associated with significant tumor regression when compared to lesions that are not accompanied by vitiligo. A trend toward further tumor regression is observed after *HSP70i*$_{Q435A}$ treatment, and treatment might impair recruitment of T cells.

We proposed that HSP70i overexpression will elicit humoral responses to the protein (Mosenson et al., 2013b). We found significant systemic responses to HSP70i in mice, yet circulating porcine anti-HSP70i titers did not reveal an increase after *HSP70i*$_{Q435A}$ application. Though local doses are high, the amount of DNA applied to swine is relatively less than what mice received. The latter is about 3-fold higher (5 μg DNA/25 g body weight compared to 5 μg of DNA/75 kg). This difference may in part account for unchanged anti-HSP70i titers in swine, or existing anti-HSP70 antibody titers are already sufficient to support anti-melanoma responses (Gunther et al., 2015) in Sinclair swine. One animal with significant melanoma burden at euthanasia did reveal a spike in anti-HSP70 titers, but was not treated with DNA. Increased titers were more likely elicited by the tumor tissue itself.

These data suggest that HSP70i$_{Q435A}$ did not interfere with cellular anti-tumor responses. Indeed, intratumoral T-cell numbers do not differ after treatment.

The culture of melanoma cells from swine skin has been reported (Gossett et al., 1996). We also generated melanoma cells from DNA-treated skin, indicating that live tumor cells continue to exist.

Importantly, jet-injected DNA induced repigmentation at distant locations as well. Thus, distant effects do occur. Limitations to these studies are primarily the number of available swine, which does not allow us to differentiate between animals of either sex, though vitiligo displays a slight sex bias (Zhang et al., 2016). Furthermore, the follow-up period is limited to 6 months; animals may ultimately undergo further depigmentation. We observed further repigmentation of a single treated lesion that was followed for an additional 6 months, repigmenting just over 30% in the first period, reaching 85% after 1 year. Finally, depigmentation does not stress the animals, whereas disease development is stressful in humans (Salzes et al., 2016).

The specimens derived from these studies provide a unique resource to study the process of vitiligo repigmentation (Birlea et al., 2017) in human-like skin.

Yet the primary observation remains that treatment with HSP70i$_{Q435A}$-encoding DNA induced repigmentation of treated and distant vitiligo lesions in Sinclair swine. An Investigational New Drug application will be required and further toxicity studies are mandatory before clinical studies can begin. Although the currently proposed DNA treatment was uniquely developed with vitiligo patients in mind, other therapeutics might ultimately demonstrate equal or superior efficacy (Rodrigues et al., 2017). On the other hand, the DNA-based treatment studied here may find applications well beyond vitiligo itself. Taken together, this study represents an important step toward a clinical application of HSP70i$_{Q435A}$ encoding DNA for the treatment of vitiligo in humans.

MATERIALS AND METHODS

Study design

S-1 Sinclair miniature swine of either sex with regressing melanomas were purchased from Sinclair BioResources (Auxvasse, MI) at 3–14 months of age and fed ad libitum. These swine develop progressive depigmentation and can manifest uveitis associated with lymphocytic infiltrates (Misfeldt and Grimm, 1994; Richerson et al., 1989). Animals were treated weekly for 4 weeks with PBS sans calcium or magnesium (n = 5 lesions on 5 swine; 2 males and 3 females) (Fisher Scientific, Pittsburgh, PA) or HSP70i$_{Q435A}$-encoding pUMVC3 plasmid DNA (n = 7 lesions on 6 swine; 2 males and 4 females) (University of Michigan Vector Core, Ann Arbor, MI) generated under Good Manufacturing Practice conditions (Aldevron, Fargo, ND). The subjects involved in each analysis are tabulated in Supplementary Table S1 (online). When multiple lesions ≥25 cm^2 were available for treatment, swine were initially subjected to PBS followed by DNA treatment 6 months later. Treated swine were transported in a sling (Lomir Biomedical, Inc., Quebec, Ontario, Canada) and anesthetized by isoflurane inhalation (Patterson Veterinary, St. Paul, MN).

Pharmajet needle-less injectors (Golden, CO) were used to introduce DNA into perilesional borders of vitiligo-affected skin. Two swine were treated with weekly doses of 2.5 mg total DNA without adverse events. Swine treated thereafter received four individual 0.5-ml doses of plasmid DNA at 2.5 mg/ml or PBS weekly for 4 weeks and were observed for 6 months thereafter. Animal studies were approved by the Northwestern and Loyola Institutional Animal Care and Use Committees and conducted according to the National Institutes of Health Guide for the Care and Use of Laboratory Animals. As shown in the figures, animals were evaluated for 27 weeks total, including the periods of treatment and follow-up. There were no outliers excluded based on Grubbs′ outlier test. For blinded analysis, vitiligo and melanoma images appeared on the screen in random order within the ImageJ macro (National Institutes of Health, Bethesda, MD).

Sample collection

Bilateral, 4-mm punch biopsies (Acuderm Inc., Fort Lauderdale, FL) were collected from perilesional skin of treated and untreated lesions before treatment and every month thereafter for 6 months. One biopsy was from the treated lesion and another preferably from a lesion within an equivalent anatomical area. Tissues were snap-frozen in optimal cutting temperature (OCT) (Sakura Finetek, Torrance, CA). Blood was collected from the subclavian/pre-cava or saphenous vein twice monthly. Ten to thirty milliliters were collected into Vacutainer tubes, and clotted blood was spun to collect serum stored at −20°C until use.

Immunohistology

Eight-micrometer cryosections were fixed in cold acetone and subjected to immunoenzymatic or immunofluorescent staining. Ten percent swine serum in Tris-buffered saline (Sigma Aldrich) was used to block aspecific binding before incubating with primary and/or labeled secondary antibodies. Antibodies used include Ta99 to TRP-1 expressed by melanocytes and melanoma cells (Thomson et al., 1985; unlabeled, mouse monoclonal; Covance, Princeton, NJ). Other primary antibodies were PPT3 to swine CD3-ε (unlabeled, mouse monoclonal; Abcam, Cambridge, MA), 76-2-11 to swine CD8-α (fluorescein isothiocyanate–labeled, mouse monoclonal; Abcam), WC1 monoclonal mouse anti-porcine γδ TCR (Abcam), polyclonal rabbit anti-porcine TGF-β latency–associated protein (Novus, Littleton, CO), SPA-810 mouse monoclonal anti-HSP70/HSP72 (Enzo Life Sciences, Farmingdale, NY), and polyclonal rabbit anti-FoxP3 (Invitrogen, Grand Island, NY). Secondary antibodies included anti-mouse IgG horseradish peroxidase–labeled antibody (SouthernBiotech, Birmingham, AL), anti-mouse IgG1 phycoerythrin-labeled antibody (Southern Biotech), anti-mouse IgG2a AF488-labeled antibody (Invitrogen), AF488-labeled anti-rabbit antibody (Invitrogen) alternating with fluorescein isothiocyanate–labeled anti-rabbit antibody (Southern Biotech). Immunohistochemical stains were developed with amino-ethylcarbazole substrate solution (Abcam), counterstaining with hematoxylin as warranted (Sigma-Aldrich) and coverslipped with Glycergel mounting medium (Dako, Glostrup, Denmark). Immunofluorescent stains to CD3 and CD8 were coverslipped with antifade reagent containing DAPI (Invitrogen, Waltham, MA). TRP-1–expressing cells were mapped across the length of the epidermis. Imaging was performed using light microscopy (Nikon, Shinagawa, Japan), and analyzed using Adobe Photoshop software (Adobe Systems

Inc., San Jose, CA). CD4 T cells were estimated as $CD3^+CD8^-$ cells to establish CD4/CD8 ratios.

Intradermal DNA application

Swine skin was shaved and scrubbed with a topical antiseptic bactericide (Betadine, Purdue Pharma L.P., Stamford, CT) and cut into 4 × 8-cm pieces. One was left untreated, and 2 others were treated with 250 μg of a pLVX-based lentiviral vector encoding ZsGreen1 (Clontech, Mountain View, CA). Jet injection (Pharmajet) or a 0.25-mm titanium microneedle dermaroller (TMT; SkinMedix, Naples, FL) were used to administer 500 μl DNA, pipetting the solution onto the skin before microneedling. Four-millimeter punch biopsies were collected and maintained in a 0.4-μm filter Transwell (Corning Star Inc., Corning, NY) atop RPMI 1640 (Fisher Scientific), 10% human serum AB (Gemini Bio Products, Sacramento, CA), L-glutamine, and antibiotics (penicillin, streptomycin, and amphotericin; Invitrogen) for 4 days. Biopsies were minced and incubated in collagenase type IV (Sigma Aldrich) and DNaseI (Sigma Aldrich). A single-cell suspension was analyzed for ZsGreen expression on a Fortessa LTR II instrument (BD Biosciences, San Jose, CA). Data were analyzed with FlowJo software (TreeStar Inc. Ashland, OR).

Repigmentation analysis

Raw images were prepared every other week using a Nikon D5300 DSLR camera (Nikon, Tokyo, Japan) under consistent lighting conditions and camera settings, including a grayscale ruler. Images were uploaded into ImageJ, and a macro was prepared to draw lassos and calculate the vitiligo and melanoma lesional areas.

ELISA

High-sensitivity ELISA kits were applied according to manufacturer′s specifications (Enzo Life Sciences, Farmingdale, NY) to detect HSP70i or anti-HSP70 IgG/A/M antibody titers in 6 monthly serum samples. Briefly, samples were added to coated ELISA plates. Washed plates were incubated with the manufacturer′s detection antibody or, for anti-HSP70 detection, with a polyclonal goat anti-swine horseradish peroxidase–conjugated antibody (Santa Cruz, CA) followed by horseradish peroxidase development of the added 3, 3′, 5, 5′-tetramethylbenzidine substrate. Plates were read in an Epoch microplate photospectrometer (BioTek, Winooski, VT) at 450 nm.

Statistical analysis

Data are shown as means ± standard error of mean, unless otherwise indicated. Experiments were performed at least twice, showing combined data or a representative experiment as appropriate. To compare trends over time for the vitiligo and melanoma lesional area analysis, a random effects linear model constrained to go through the origin was used, with lesion as a random effect and time as a fixed effect. For fluorocytometry, immunohistology and ELISA data, *t* tests allowing for unequal variance were used. Degrees of freedom for two-sample *t* tests were calculated with Satterthwaite's formula. Two-sided tests were performed except where an expected increase or decrease was evaluated, and *t* tests were

calculated with Excel software (Microsoft, Redmond, WA). Graphs were made with Prism software (GraphPad Software). *P* values <0.05 were considered statistically significant.

Supplementary Material

Refer to Web version on PubMed Central for supplementary material.

ACKNOWLEDGEMENTS

Sinclair Bioresources is acknowledged for careful prescreening and handling of animals. We appreciate help from Levi Barse to generate a macro that measures lesional area. All authors corrected and approved of the manuscript. Funding was provided by National Institutes of Health/National Institute of Arthritis and Musculoskeletal and Skin Diseases grant 1R44AR065866 to AS and by National Institutes of Health/National Cancer Institute grant R01CA191317 to CLP. International Patent Application No. PCT/US12/53139 was filed related to the application of *HSP70i*^{Q435A} to treat autoimmune disease.

CONFLICT OF INTEREST

These studies were supported in part by NIH funding for an SBIR phase I study to Radikal Therapeutics.

Abbreviations:

DC	dendritic cell
HSP70i	inducible HSP70
PBS	phosphate buffered saline

REFERENCES

Abdou AG, Maraee AH, Reyad W. Immunohistochemical expression of heat shock protein 70 in vitiligo. Ann Diagn Pathol 2013;17:245–9. [PubMed: 23352325]

Apostolopoulos V. Vaccine delivery methods into the future. Multidisciplinary Digital Publishing Institute (MDPI). Vaccines 2016;4(2).

Becker JC, Guldberg P, Zeuthen J, Brocker EB, Straten PT. Accumulation of identical T cells in melanoma and vitiligo-like leukoderma. J Invest Dermatol 1999;113:1033–8. [PubMed: 10594748]

Birlea SA, Costin GE, Roop DR, Norris DA. Trends in regenerative medicine: repigmentation in vitiligo through melanocyte stem cell mobilization. Med Res Rev 2017;37:907–35. [PubMed: 28029168]

Blangero J, Tissot RG, Beattie CW, Amoss MS Jr. Genetic determinants of cutaneous malignant melanoma in Sinclair swine. Br J Cancer 1996;73: 667–71. [PubMed: 8605105]

Boniface K, Jacquemin C, Darrigade AS, Dessarthe B, Martins C, Boukhedouni N, et al. Vitiligo skin is imprinted with resident memory CD8 T cells expressing CXCR3. J Invest Dermatol 2018;138:355–64. [PubMed: 28927891]

Bourneuf E. The MeLiM Minipig: an original spontaneous model to explore cutaneous melanoma genetic basis. Front Genet 2017;8:146. [PubMed: 29081790]

Duan B, Cheng L, Gao Y, Yin FX, Su GH, Shen QY, et al. Silencing of fat-1 transgene expression in sheep may result from hypermethylation of its driven cytomegalovirus (CMV) promoter. Theriogenology 2012;78: 793–802. [PubMed: 22541322]

Frisoli ML, Harris JE. Vitiligo: mechanistic insights lead to novel treatments. J Allergy Clin Immunol 2017;140:654–62. [PubMed: 28778794]

Gossett R, Kier AB, Schroeder F, McConkey D, Fadok V, Amoss MS Jr. Cycloheximide-induced apoptosis in melanoma cells derived from regressing cutaneous tumours of Sinclair swine. J Comp Pathol 1996;115:353–72. [PubMed: 9004078]

Gunther S, Ostheimer C, Stangl S, Specht HM, Mozes P, Jesinghaus M, et al. Correlation of Hsp70 serum levels with gross tumor volume and composition of lymphocyte subpopulations in patients with squamous cell and adeno non-small cell lung cancer. Front Immunol 2015;6:556. [PubMed: 26579130]

Harris JE. Cellular stress and innate inflammation in organ-specific autoimmunity: lessons learned from vitiligo. Immunol Rev 2016;269:11–25. [PubMed: 26683142]

Jacquemin C, Rambert J, Guillet S, Thiolat D, Boukhedouni N, Doutre MS, et al. Heat shock protein 70 potentiates interferon alpha production by plasmacytoid dendritic cells: relevance for cutaneous lupus and vitiligo pathogenesis. Br J Dermatol 2017;177:1367–75. [PubMed: 28380264]

Jung EC, Maibach HI. Animal models for percutaneous absorption. J Appl Toxicol 2015;35:1–10. [PubMed: 25345378]

Kim YC, Jarrahian C, Zehrung D, Mitragotri S, Prausnitz MR. Delivery systems for intradermal vaccination. Curr Topics Microbiol Immunol 2012;351:77–112.

Kundu RVM, Mhlaba JM, Rangel SM, Le Poole IC. The convergence theory for vitiligo: a reappraisal. Exp Dermatol 2018 Apr 28. 10.1111/exd.13677 [Epub ahead of print].

Le Poole IC, van den Wijngaard RM, Westerhof W, Dutrieux RP, Das PK. Presence or absence of melanocytes in vitiligo lesions: an immunohisto-chemical investigation. J Invest Dermatol 1993;100:816–22. [PubMed: 7684427]

Liao S, Lv J, Zhou J, Kalavagunta PK, Shang J. Effects of two chronic stresses on mental state and hair follicle melanogenesis in mice. Exp Dermatol 2017;26:1083–90. [PubMed: 28480983]

Mantovani S, Garbelli S, Palermo B, Campanelli R, Brazzelli V, Borroni G, et al. Molecular and functional bases of self-antigen recognition in long-term persistent melanocyte-specific CD8+ T cells in one vitiligo patient. J Invest Dermatol 2003;121:308–14. [PubMed: 12880423]

Misfeldt ML, Grimm DR. Sinclair miniature swine: an animal model of human melanoma. Vet Immunol Immunopathol 1994;43:167–75. [PubMed: 7856049]

Morgan CD, Measel JW Jr, Amoss MS Jr, Rao A, Greene JF Jr. Immunophenotypic characterization of tumor infiltrating lymphocytes and peripheral blood lymphocytes isolated from melanomatous and non-melanomatous Sinclair miniature swine. Vet Immunol Immunopathol 1996;55:189–203. [PubMed: 9014317]

Mosenson JA, Eby JM, Hernandez C, Le Poole IC. A central role for inducible heat-shock protein 70 in autoimmune vitiligo. Exp Dermatol 2013a;22:566–9. [PubMed: 23786523]

Mosenson JA, Flood K, Klarquist J, Eby JM, Koshoffer A, Boissy RE, et al. Preferential secretion of inducible HSP70 by vitiligo melanocytes under stress. Pigment Cell Melanoma Res 2014;27:209–20. [PubMed: 24354861]

Mosenson JA, Zloza A, Klarquist J, Barfuss AJ, Guevara-Patino JA, Le Poole IC. HSP70i is a critical component of the immune response leading to vitiligo. Pigment Cell Melanoma Res 2012;25:88–98. [PubMed: 21978301]

Mosenson JA, Zloza A, Nieland JD, Garrett-Mayer E, Eby JM, Huelsmann EJ, et al. Mutant HSP70 reverses autoimmune depigmentation in vitiligo. Sci Transl Med 2013b;5(174):174ra28.

Naveh HP, Rao UN, Butterfield LH. Melanoma-associated leukoderma—immunology in black and white? Pigment Cell Melanoma Res 2013;26:796–804. [PubMed: 24010963]

Ogg GS, Rod Dunbar P, Romero P, Chen JL, Cerundolo V. High frequency of skin-homing melanocyte-specific cytotoxic T lymphocytes in autoimmune vitiligo. J Exp Med 1998;188:1203–8. [PubMed: 9743539]

Okomo-Adhiambo M, Rink A, Rauw WM, Gomez-Raya L. Gene expression in Sinclair swine with malignant melanoma. Animal 2012;6:179–92. [PubMed: 22436175]

Richerson JT, Burns RP, Misfeldt ML. Association of uveal melanocyte destruction in melanoma-bearing swine with large granular lymphocyte cells. Invest Ophthalmol Vis Sci 1989;30:2455–60. [PubMed: 2592158]

Richmond JM, Masterjohn E, Chu R, Tedstone J, Youd ME, Harris JE. CXCR3 depleting antibodies prevent and reverse vitiligo in mice. J Invest Dermatol 2017;137:982–5. [PubMed: 28126463]

Rodrigues M, Ezzedine K, Hamzavi I, Pandya AG, Harris JE. Current and emerging treatments for vitiligo. J Am Acad Dermatol 2017;77:17–29. [PubMed: 28619557]

Salzes C, Abadie S, Seneschal J, Whitton M, Meurant JM, Jouary T, et al. The Vitiligo Impact Patient Scale (VIPs): development and validation of a vitiligo burden assessment tool. J Invest Dermatol 2016;136:52–8. [PubMed: 26763423]

Shevtsov M, Huile G, Multhoff G. Membrane heat shock protein 70: a theranostic target for cancer therapy. Philos Trans R Soc Lond B Biol Sci 2018;373(1738).

Sosa JJ, Currimbhoy SD, Ukoha U, Sirignano S, O'Leary R, Vandergriff T, et al. Confetti-like depigmentation: a potential sign of rapidly progressing vitiligo. J Am Acad Dermatol 2015;73:272–5. [PubMed: 26054430]

Strassner JP, Harris JE. Understanding mechanisms of autoimmunity through translational research in vitiligo. Curr Opin Immunol 2016;43:81–8. [PubMed: 27764715]

Thomson TM, Mattes MJ, Roux L, Old LJ, Lloyd KO. Pigmentation-associated glycoprotein of human melanomas and melanocytes: definition with a mouse monoclonal antibody. J Invest Dermatol 1985;85:169–74. [PubMed: 3926906]

Wańkowicz-Kalińska A, van den Wijngaard RM, Tigges BJ, Westerhof W, Ogg GS, Cerundolo V, et al. Immunopolarization of CD4+ and CD8+ T cells to Type-1-like is associated with melanocyte loss in human vitiligo. Lab Invest 2003;83:683–95. [PubMed: 12746478]

Zhang Y, Cai Y, Shi M, Jiang S, Cui S, Wu Y, et al. The prevalence of vitiligo: a meta-analysis. PLoS One 2016;11:e0163806. [PubMed: 27673680]

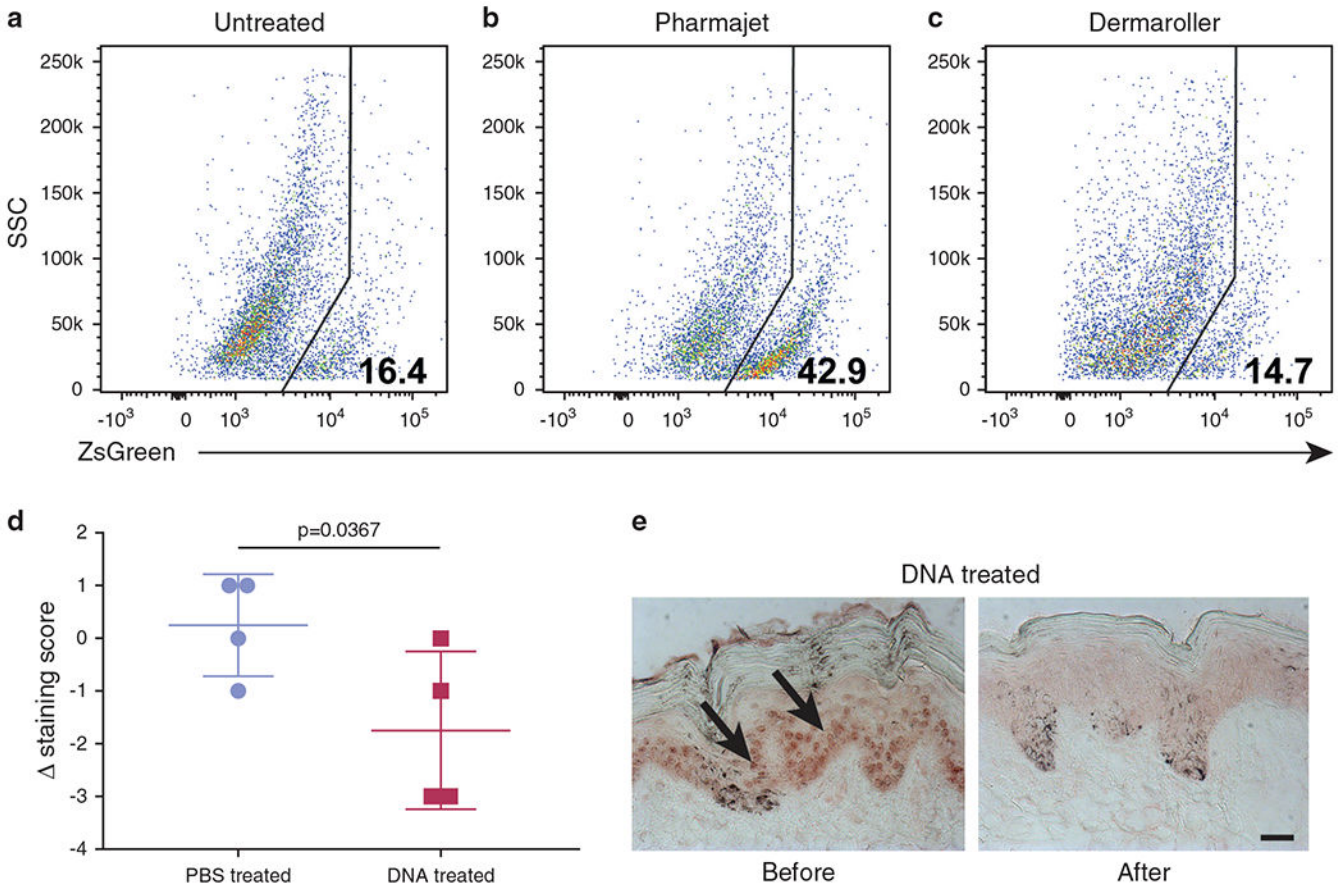

Figure 1. Jet injection of HSP70i$_{Q435A}$-encoding DNA can suppress nuclear expression of the HSP in perilesional vitiligo skin.

Fluorescent protein ZsGreen expression from an expression plasmid was compared between (**a**) untreated skin, (**b**) jet injected and (**c**) microneedle introduction of similar amounts of DNA followed by tissue homogenization after 96 hours and fluorocytometry. (**d**) Significantly reduced nuclear expression of HSP70i was observed in n = 4 perilesional samples of DNA compared to vehicle-treated skin, comparing epidermal expression before (t = 0) and at the end (t = 3 weeks) of treatment. (**e**) Example of reduced nuclear HSP70i expression. Scale bar = 25 μm. HSP70i$_{Q435A}$, inducible HSP70$_{Q435A}$.

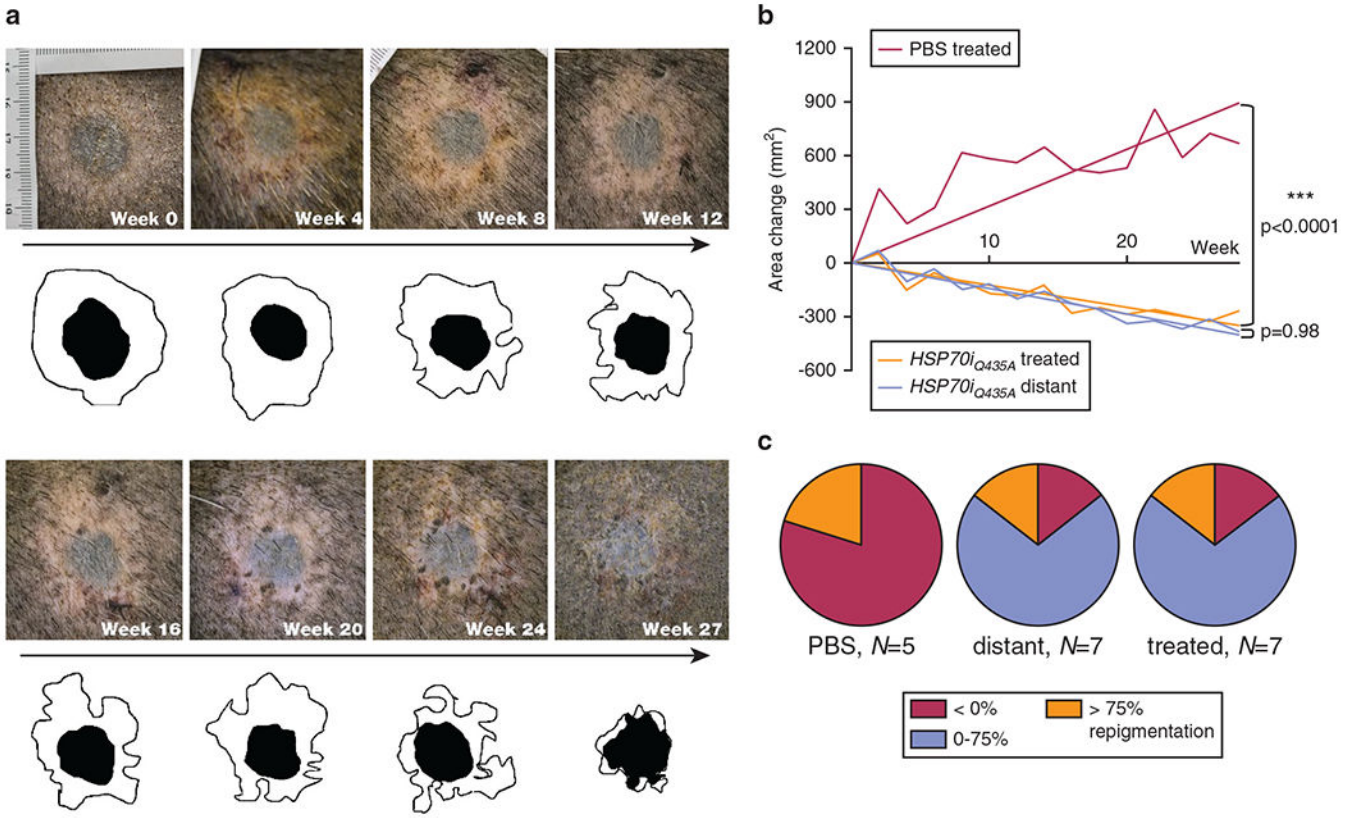

Figure 2. *HSP70i*$_{Q435A}$ can drive repigmentation of vitiligo lesions in Sinclair swine.

(**a**) An example (DNA-treated) vitiligo lesion that has developed around a melanoma tumor is followed over time using a lasso and image analysis to quantify the area of depigmentation (outer margins shown). (**b**) significant repigmentation is observed in seven vitiligo lesions treated with HSP70i$_{Q435A}$- encoding DNA, as well as seven distant lesions, each compared to five PBS-treated lesions from separate swine (slopes −12.5, −14.2, and +31.9, respectively; $P < 0.0001$ for both comparisons). The straight lines display the slopes calculated from the underlying data, which are shown as the mean change in lesional area at each time point. (**c**) Represented as repigmentation in percentage increments, repigmentation was observed in the majority of treated and distant lesions whereas vehicle treated lesions primarily depigmented over time. HSP70i$_{Q435A}$, inducible HSP70$_{Q435A}$; PBS, phosphate buffered saline.

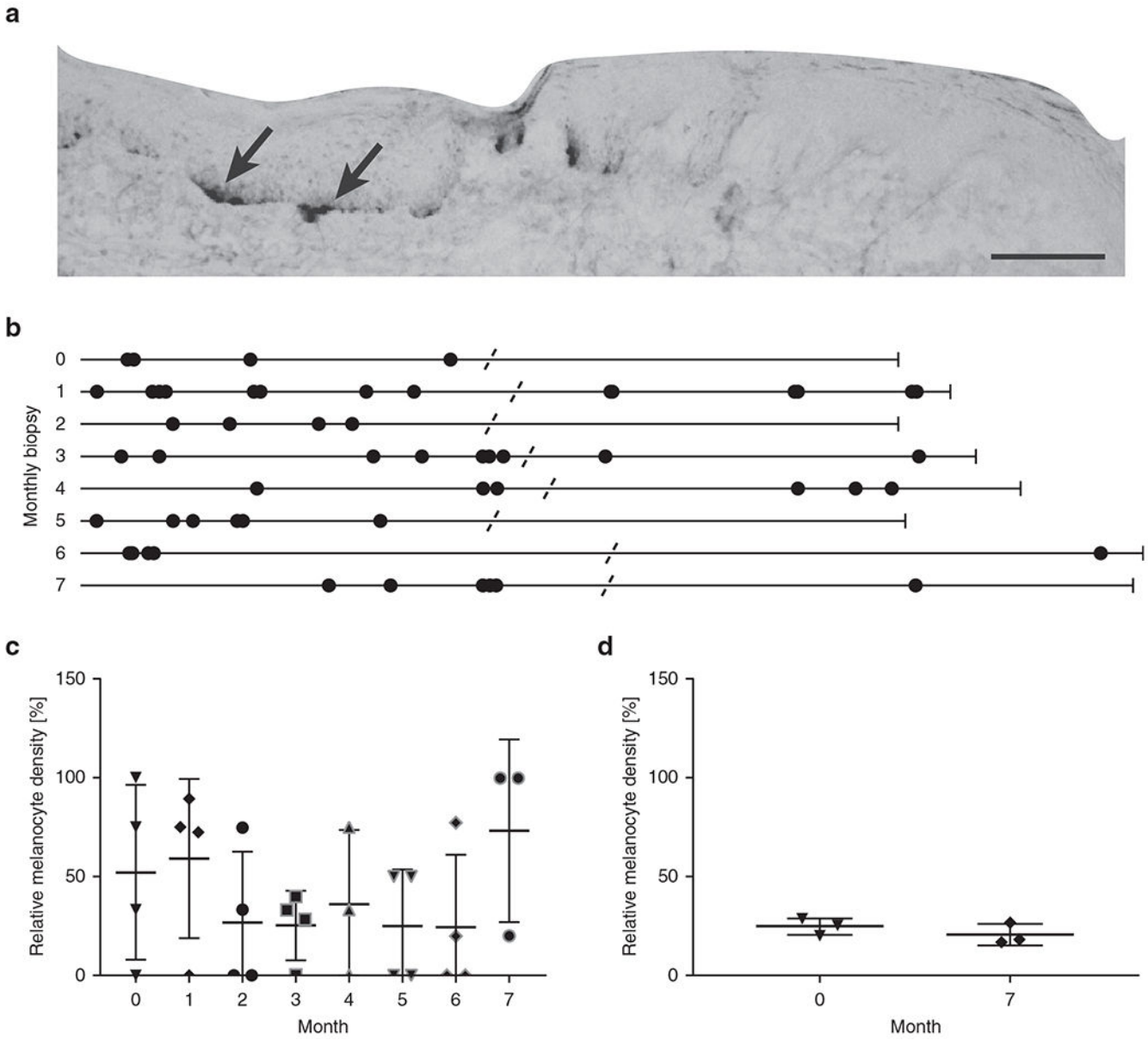

Figure 3. Melanocytes are found in repigmenting perilesional skin.

Biopsies were carefully oriented to cover 50:50 melanized and depigmented skin before sectioning and staining. (**a**) Example TRP-1 staining showing melanocytes in the pigmented section of perilesional skin; enlarged image shows part of a section. Scale bar = 100 μm. (**b**) Melanocyte distribution in monthly perilesional biopsies from one repigmenting lesion. TRP-1–expressing cells are displayed as dots on a straightened line that represents the length of the epidermis. TRP-1 staining spanning the breadth of most biopsies suggests that some melanocytes are present before visible repigmentation. (**c**) Relative melanocyte density in DNA-treated skin (n = 4) over time in the depigmented:pigmented section of each biopsy ×100%. (**d**) The same parameter measured in untreated perilesional skin (n = 4) at the beginning and end point of follow-up suggests that some melanocytes are present beyond the border of pigmented skin independent of disease progression status.

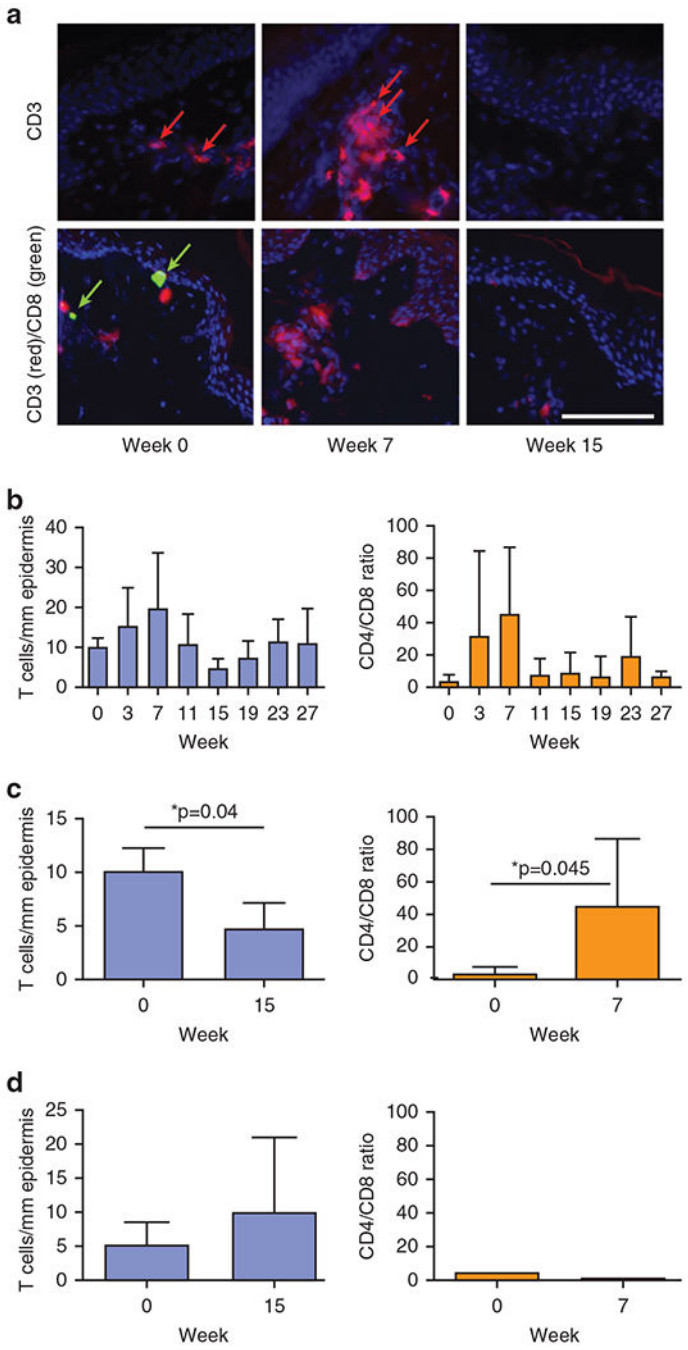

Figure 4. T-cell infiltrates are reduced 3 months after *HSP70i*$_{Q435A}$ treatment.

T-cell infiltrates were evaluated in perilesional tissue sections. (**a**) Sample stainings for CD3 alone and for CD3 and CD8 are shown at different time points, the latter performed to establish CD4:CD8 ratios. Single stained cells are counted as $CD4^+$. Scale bar = 100 μm. (**b**) In violet, quantification of total T-cell infiltrates over time in repigmenting skin biopsies (n = 4) expressed per epidermal length, with densities initially trending toward an increase followed by a significant decrease by week 15. In orange, CD4:CD8 ratios (n = 4) follow the same trend as CD8 T cells alone. (**c**) A significant decrease in T cells is found during

repigmentation of DNA-treated lesions, whereas a significant increase in the CD4/CD8 ratio at week 7 suggests that fluctuations follow the CD4 subset rather than cytotoxic T cells. (**d**) By contrast, the number of infiltrating T cells in vehicle-treated skin (n = 3) does not vary from the pretreatment numbers also observed in DNA-treated lesions. $HSP70i_{Q435A}$, inducible $HSP70_{Q435A}$.

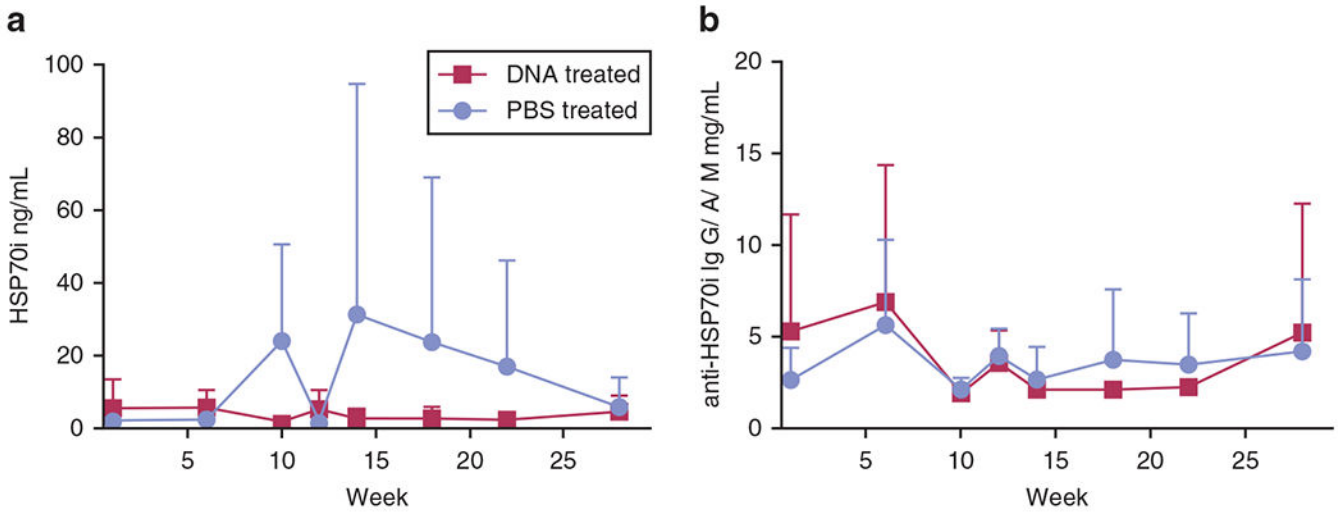

Figure 5. Systemic humoral responses are not significantly affected by HSP70-encoding DNA.

Sequential serum samples obtained from six sample sets of DNA-treated swine and seven sample sets of PBS control swine displayed (**a**) no increase in HSP70 titers in response to HSP70i$_{Q435A}$-encoding DNA (magenta) compared to PBS-treated swine (violet) and (**b**) no significant fluctuations in anti-HSP70 titers; an initial spike after treatment cannot be assigned to HSP70-encoding DNA. HSP70i$_{Q435A}$, inducible HSP70$_{Q435A}$; PBS, phosphate buffered saline.

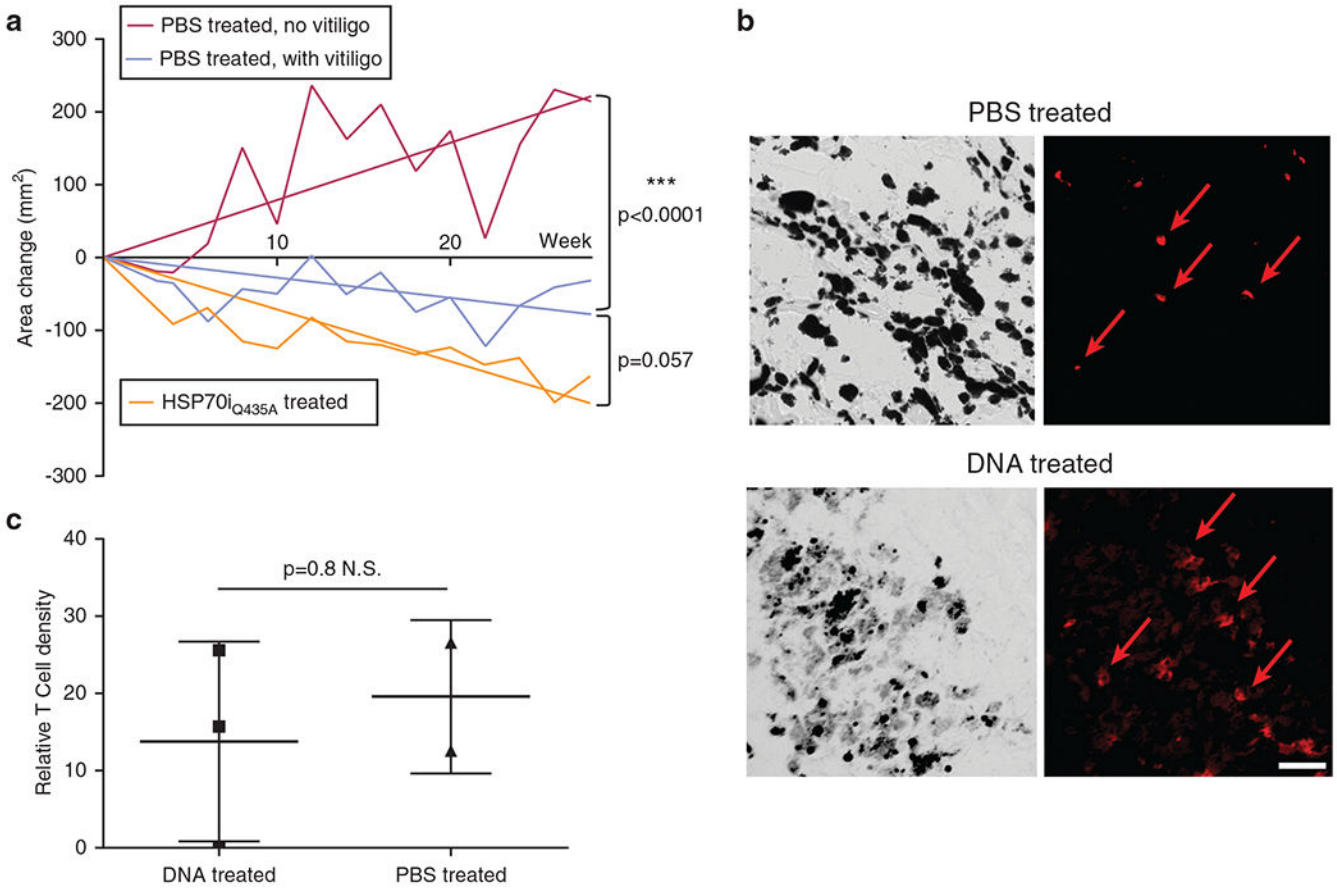

Figure 6. HSP70i treatment does not increase the risk of melanoma outgrowth.

(**a**) Surface area was measured for melanomas central to HSP70i$_{Q435A}$-treated vitiligo lesions (orange, n = 7) or PBS-treated lesions (violet if accompanied by vitiligo, n = 4 and magenta if not, n = 3). The straight line displays the slope calculated from the underlying data, which are shown as the mean change in lesional area at each time point. The slope for DNA treated skin was −8 mm^2; for PBS-treated skin it was −3 (vitiligo) or 5 mm^2 (no vitiligo). Though lesions shrunk significantly faster following DNA versus PBS treatment overall, this is largely due to the presence of vitiligo ($P < 0.0001$). DNA treatment resulted in the greatest negative slope, and it is clear HSP70i$_{Q435A}$ did not impair tumor immune surveillance. (**b**) Examples of CD3 staining used for T-cell quantification. T-cell staining (arrows) shown for melanomas amidst a PBS-treated and a DNA-treated lesion. Brightfield and fluorescent images shown. Scale bar = 100 μm. (**c**) T-cell density was quantified at end point with no evidence that DNA treatment affects T-cell infiltration in tumors. HSP70i$_{Q435A}$, inducible HSP70$_{Q435A}$; PBS, phosphate buffered saline.